

RESEARCH

Open Access



Enhancing the clinical diagnosis of the acute and subacute phases of autoimmune encephalitis and predicting the risk factors: the potential advantages of 18F-FDG PET/CT

Lili Liu^{1†}, Zhehao Lyu^{2†}, Huimin Li³, Lin Bai¹, Yong Wan¹ and Ping Li^{1*}

Abstract

Background 2-deoxy-2-[18F]fluoro-D-glucose positron emission tomography (18F-FDG PET) could help evaluate metabolic abnormalities by semi-quantitative measurement to identify autoimmune encephalitis (AE). Few studies have been conducted to analyze the prognostic factors of AE. The study aimed to explore the values of diagnosis and treatment evaluation by 18F-FDG PET and preliminarily discussed the potential value in predicting the prognosis of AE patients.

Methods AE patients underwent 18F-FDG PET/CT and magnetic resonance imaging (MRI). There were two steps to analyse 18F-FDG PET imaging data. The first step was visual assessment. The second step was to analyse 18F-FDG PET parameters using Scenium software (Siemens Molecular Imaging Ltd). The mean standardized uptake value (SUV_{mean}) and maximum standardized uptake value (SUV_{max}) of brain relative regional metabolism (BRRM) were quantified in the case and control groups according to the anatomical automatic labeling (AAL) partition. The main statistical method was the Kruskal–Wallis test. Finally, the simple linear regression method was used to analyse the relationships between 18F-FDG PET parameters and the modified Rankin Scale (mRS) scores before and after treatment.

Results The results on 18F-FDG PET showed that visual assessment abnormalities were in the mesial temporal lobe (MTL) (70.8%), (mainly infringing on the hippocampus and amygdala), basal ganglia (62.5%), frontal lobes (37.5%), occipital lobes (29.2%), and parietal lobes (12.5%). The positive rate of abnormalities on 18F-FDG PET was more sensitive than that on MRI (95.5% vs 32.2%, $p=0.001$). The number of lesions on PET was positively correlated with the mRS scores before and after treatment, and the correlation before treatment was more significant. Before treatment, the SUV_{mean} of the left occipital lobe was the most remarkable (SUV_{mean} , $R^2=0.082$, $p>0.05$) factor associated with the mRS score, and the correlation was negative. With regard to prognosis, the SUV_{max} of the MTL was the most notable ($R^2=0.1471$, $p>0.05$) factor associated with the mRS score after treatment, and the correlation was positive.

Conclusions 18F-FDG PET could be more sensitive and informative than MRI in the early phases of AE. The common pattern of AE was high MTL metabolism on 18F-FDG PET, which was associated with hypometabolism of the occipital

[†]Lili Liu and Zhehao Lyu contributed equally to this paper.

*Correspondence:

Ping Li

pinglihmu@yahoo.com

Full list of author information is available at the end of the article



lobe, and the number of lesions on PET before treatment may be significant factors in assessing disease severity. The SUV_{max} of MTL hypermetabolism may serve as a prognostic biomarker in AE.

Keywords Autoimmune encephalitis, 18F-FDG PET/CT, Clinical diagnosis, Risk factors

Background

Autoimmune encephalitis (AE) is a non-infectious, immune-mediated inflammatory disease of the cerebrum parenchyma; this subacute presentation is highlighted in the Graus criteria and is a hallmark of the disorder, which is different from acute encephalitis developing as a rapidly progressive encephalopathy (usually in less than 6 weeks) [1–5]. Recent studies have found that the prevalence was 13.7 per 100,000 in Europe [6]. However, the mechanism underlying AE development is still unclear. It may be triggered by herpes simplex virus (HSV) encephalitis or specific immune-modulating therapies such as immune-checkpoint inhibitors (ICIs); the former is commonly associated with some common preceding factors such as viral infection, fever, or viral-like prodrome at the onset of this disorder [7], and the latter could result from an accelerated form of paraneoplastic encephalitis with advanced cancers [8]. The pace of disease progression may include acute and subacute presentations, and the median time from symptom onset to clinical assessment usually lasts several weeks [9, 10]. As noted, an individual may seem to have a precipitous deterioration concerning AE, but after further history-taking, it becomes apparent that there has been milder cognitive impairment over months or even years [11].

Imaging examinations of AE are based on magnetic resonance imaging (MRI), which can rule out stroke, tumours, and other infectious encephalitides. 2-deoxy-2-[18F] fluoro-D-glucose positron emission tomography (18F-FDG PET) is used as an auxiliary tool to be performed with more sensitivity and information related to brain abnormalities [12] when the results are negative or patients have contraindications for MRI. On the basis of background conditions, we conducted semi-quantitative analysis of 18F-FDG PET to verify the metabolic characteristics and to explore prognostic factors of AE.

Methods

Patients

A total of 32 patients with AE were retrospectively reviewed from the Second and First Affiliated Hospitals of Harbin Medical University between January 2017 and June 2022. All patients fulfilled the clinical diagnostic criteria and were positive for AE-related antibodies in the serum or cerebrospinal fluid (CSF). Thirty-one patients underwent MRI, and 24/31 patients underwent 18F-FDG

PET (both anti-GAD65 and anti-LGI1 patients were re-examined after treatment in one year). Neuroimaging examinations (all MRIs and the remaining 22 patients' PETs) were carried out in the acute and subacute stages after symptom onset. For the group analysis of 18F-FDG PET imaging, we identified 101 healthy controls without neurological anomalies, dividing them into two groups (Fig. 1) [13]. The 19 to 44-year-old group was named control group-1 (9 males, 12 females, the average age of males was 34.78 ± 8.00 years old [mean \pm standard deviation, mean \pm SD] and that of females was 36.92 ± 6.69 years old). The 45 to 70-year-old group was named control group-2, including the development group (28 males, 54.25 ± 5.5 years old, 25 females, 56.0 ± 7.2 years old) and verified groups (14 males, 51.43 ± 4.3 years old, 13 females, 55.8 ± 8.0 years old).

The demographic and clinical information, laboratory test results, and electroencephalograph (EEG) findings for individual patients and the comparison of the results are presented in (Table 1).

Antibody testing

All 32 patients underwent serum and CSF antibody testing, including tests for classic paraneoplastic antibodies (Hu, Yo, Ri, Ma2, CV2, Amphiphysin) and N-methyl-D-aspartate receptor (NMDAR), leucine-rich glioma inactivated-1 (LGI1), contacting-associated protein-2 (CASPR2), gamma-aminobutyric acid receptor (GABABR), α -amino-3-hydroxy-5-methyl-4-isoxazole propionic acid receptor (AMPA), and glutamic acid decarboxylase 65 (GAD65) antibodies. Serum and CSF samples were analyzed using cell-based assays (Euroimmun, Lübeck, Germany), immunohistochemical analyses in the neuroimmunology laboratory of the Peking Union Medical College Hospital and Heilongjiang Kingmed for Clinical Laboratory.

MRI

The MRI scanner was a 3.0 Tesla Discovery 750w MRI (GE Healthcare, USA). The standard MRI protocols included T1-weighted imaging (T1WI), T2-weighted imaging (T2WI), fluid-attenuated inversion recovery (FLAIR), and diffusion-weighted imaging (DWI). For T1WI [repetition time (TR)=2203 ms, echo time (TE)=25 ms, field of view (FOV)=240 mm \times 240 mm], T2WI (TR=4356 ms, TE=90 ms, FOV=240 mm \times 240 mm), FLAIR

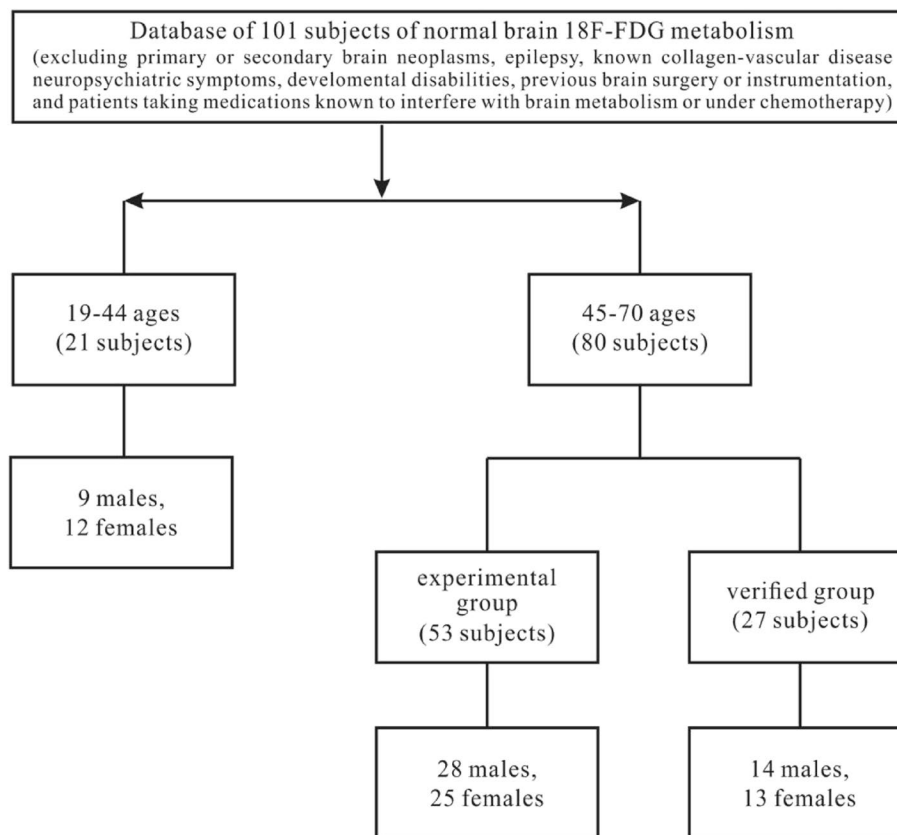


Fig. 1 The establishment of normal control group and excluding criterion. The normal data of brain was included 101 subjects, which were divided into two groups, 19–44 years old group (named control group-1) and 45–70 years old group, the latter was separated into experimental group and verified group (named control group-2)

(TR=6525 ms, TE=83 ms, FOV=240 mm×240 mm), and DWI (TR=3686 ms, TE=77 ms, FOV=240 mm×240 mm), axial images were obtained, and the slice thickness was 5 mm. Two experienced radiologists independently evaluated the MRI results. If there was obvious discordance at the beginning of the evaluations, an informed consensus was achieved.

18F-FDG PET/CT

The PET/CT scanner was a Siemens Biograph 64 time-of-flight scanner. All patients were asked to fast for at least 6 h, and fasting blood glucose levels could not exceed 8 mmol/L. The injection dose was 0.12 mCi/kg, and the imaging agent was 18F-FDG. After injection, they were required to rest quietly and were isolated in a dedicated room to ensure minimal auditory and visual stimulation. The brain and whole-body imaging acquisition time was 40 min after injection. The brain acquisition time was 3 min/bed, and the speed of the whole body acquisition was 1.5 mm/s. Slice thickness was 3 mm and 1 mm.

Analysis of 18F-FDG PET imaging

Visual assessment and Scenium software methods in case and control groups

Visual assessment was performed by two board-certified radiologists (10 years). 18F-FDG PET image analysis should be performed by drawing the region of interest (ROI) and then calculating the SUV and asymmetric index (AI) [14]:

$$AI = \frac{2 \times (SUV(ipsilateral) - SUV(contralateral))}{SUV(ipsilateral) + SUV(contralateral)}$$

If the value of AI was larger than the threshold (e.g., 0.15) for three consecutive slices, the focus was determined to be a metabolic abnormality [15]. Encephalitis was suspected if there were manifestations of numerous focal cortical and/or subcortical abnormalities on MRI and hyper and/or hypometabolism on 18F-FDG PET. Scenium software provides quantification tools for the assessment of FDG-PET to calculate a statistical analysis of patients versus normal subjects and colour-coded statistical analysis, highlighting patterns

Table 1 Clinical characteristics of AE patients

Item (total 32 subjects)	Anti-NMDAR	Anti-GABABR	Anti-LGI1	Anti-HU (anti-HU N=4) (anti-HUandSOX1 n=2) (anti-HU and Ri n=1)	Anti-GAD65	Anti-PNMA2 +/- Ma2/Ta	Anti-Amphiphysin	Anti-CASPR2	Anti-GFAP	P value
	N=6	N=5	N=8	N=7	N=2	N=1	N=1	N=1	N=1	
Age, years (media IQR)	24.5 {13–36}	56.8 {41–66}	59.5 {40–67}	60.5 {51–77}	59.5 {55–64}	48	63	55	35	0.005*
Female/male	4/2	1/4	4/4	6/1	2/0	0/1	0/1	0/1	1/0	0.229
Seizures	6	5	8	2	0	1	1	1	0	0.001*
Encephalalgia and dizziness	6	3	3	5	2	1	0	1	1	0.201
Decreased level of Consciousness	2	2	3	1	1	1	0	0	0	0.906
Cognitive impairment	2	3	4	2	1	1	1	0	0	0.906
Psychiatric symptoms	2	0	1	3	0	0	0	0	1	0.550
Metamorphopsia	1	0	0	2	2	0	0	0	1	0.033*
Speech disorder	2	0	1	1	0	0	0	0	1	0.811
Auditory hallucination	1	0	0	0	0	0	0	1	0	0.317
WBC ↑ (4.0–10.0 10 ⁹ /L)	3	0	5	1	2	1	0	0	0	0.052
NUET% ↑ (50.0–70.0%)	4	2	7	4	2	1	0	1	1	0.523
LYMPH% ↓ (20.0–40.0%)	3	2	6	3	2	1	0	1	1	0.598
CPR ↑ (mg/L)	4	5	7	6	2	1	0	1	1	0.811
CSF-TPC ↑ (mg/L)	2	3	4	0	1	1	1	1	1	0.021*
Abnormal EEG-the sharp and slow waves in frontal or temporal	6	5	3	-	1	0	0	1	0	0.007*
Anti-ANA spectrum: nuclear particle type 1:100	2	2	4	4	1	-	-	-	1	0.849
Tumor markers {CEA ↑ or SCC ↑ or CA125 ↑ or NSE ↑ or CYFRA21-1 ↑ or CA724 ↑, CA199 ↑}	0	2	3	5	0	-	1	1	0	0.370
Abnormal brain MRI before treatment	3	2	4	1	1	1	-	-	1	0.409
mRS scores at the time of 18F-FDG PET/CT (media IQR)	2 {1,4}	3.2 {1,4}	2.6 {1,4}	3.6 {3,4}	2.5 {2,3}	5	3	2	3	0.217
Treated with steroids before 18F-FDG PET or MRI	0	1	0	0	0	0	0	0	0	0.344
Treated with AED before 18F-FDG PET or MR	6	5	8	0	0	1	1	1	1	0.001*
First-line treatment	6	5	8	7	2	1	1	1	1	1

Table 1 (continued)

Item (total 32 subjects)	Anti-NMDAR	Anti-GABABR	Anti-LGI1	Anti-HU	Anti-GAD65	Anti-PNMA2 +/- Ma2/Ta	Anti-Amphiphysin	Anti-CASPR2	Anti-GFAP	P value
	N=6	N=5	N=8	N=7 (anti-HU N=4) (anti-HUandSOX1 n=2) (anti-HU and RI n=1)	N=2	N=1	N=1	N=1	N=1	
Long immune treatment	0	0	1	0	1	0	0	1	1	0.047*
Follow-up time {months}	14.3 {5-30}	16.7 {5-50}	15.2 {7-26}	18.9 {6-48}	15 {4-26}	42	13	16	—	0.001*
mRS at the last follow up {media IQR}	1.7 {1-3}	5 {2-6}	2.4 {0-6}	4.1 {1-6}	1 {1}	3	1	1	0	0.001*

Abbreviations: AE Autoimmune Encephalitis, 18F-FDG PET/CT 2-deoxy-2-[18F]fluoro-D-glucose positron emission tomography-computed tomography, MRI magnetic resonance imaging, mRS modified Rankin Scale, CRP C-reactive protein, CSF cerebrospinal fluid, TPC total protein counts, EEG electroencephalogram, WBC White Blood Cell, CEA Carcinoembryonic antigen, the normal value < 5 ng/mL, SCC squamous cell carcinoma antigen, the normal value < 1.5 ng/mL, CYFRA21-1 Cytokeratin-19-fragment, the normal value < 2.5 ng/mL, NSE neuron-specific enolase, the normal value < 17 ng/mL, CA125 the normal value < 35U/ml, CA199 the normal value < 37U/ml, AED anti-epileptic drugs; The first line of treatment included steroids, IVIg, and plasma exchange; Long immune treatment included Mycophenolate Mofetil and Azathioprine; The certain group: included four patients, anti-PNMA2 +/-Ma2/ta, anti-Amphiphysin, anti-CASPR2, anti-GFAP, respectively one case, however, only anti-PNMA2 +/-Ma2/ta, anti-Amphiphysin performed PET examination; NMDAR N-methyl-D-aspartate receptor, LGI1 leucine-rich glioma inactivated-1, CASPR2 contacting-associated protein-2, GABABR gamma-aminobutyric acid receptor, AMPAR α-amino-3-hydroxy-5-methyl-4-isoxazole propionic acid receptor, GAD65 glutamic acid decarboxylase 65. *p < 0.05

of unusual radiopharmaceutical uptake. This software uses a deformable fusion algorithm to fuse the patient to the normal subject image to give an accurate match for cortical structures. Minimum, maximum and mean intensity values are computed for each region together with statistical information [16]. Regions of interest are licenced from CEA/Groupe d'Imagerie Fonctionnelle [17]. The cerebrum was divided into 53 regions (excluding the cerebellum and brainstem) according to automated anatomical labelling (AAL) standards. Brain relative regional metabolism (BRRM) values of case groups, control group-1 and 2 were calculated. Excel forms were created, including data on the mean standardized uptake value (SUV_{mean}), standard deviation of the SUV_{mean} ($SUV_{meanstd}$), maximum standardized uptake value (SUV_{max}), and standard deviation of the SUV_{max} (SUV_{maxstd}) of each brain ROI [seen in Supplemental tables (1–12)]. The mean value and 95% confidence interval were obtained. Simultaneously, the whole-body PET was used to screen for tumours.

A score of 1 was given for a focal anomaly in a lobe or increased uptake in the basal ganglia, and a score of 0 was given for the absence of a lobar anomaly or increased uptake in the basal ganglia through Scenium analysis.

Follow-up and prognosis analysis

The modified Rankin Scale (mRS) scores were used to assess neurological disability at the onset and the last follow-up for this disorder. The mRS scores ≤ 2 indicated a good outcome, and the mRS scores of 3 to 6 indicated a poor outcome. The relationships among 18F-FDG PET parameters, severity degrees of the disease, and the outcome at the last follow-up after treatment were assessed.

Statistical analysis

SPSS 25.0 software package for Windows (IBM Corp) and GraphPad Prism 9.4.1 (GraphPad Software, USA) were used for statistical analysis and charts. Categorical variables were compared and analyzed by Fisher's exact test. Data are presented as the mean \pm SD for continuous variables with a normal distribution, and non-normally distributed variables are expressed as the median (interquartile range [IQR]). Continuous variables were compared using the *t* test or nonparametric Mann–Whitney U test. The Kruskal–Wallis test was used to analyze multiple groups of constant variable comparisons. The relationships between continuous variables of SUV_S (SUV_{mean} , SUV_{max}) and the mRS scores (before and after treatment) were explored by simple linear regression. A two-tailed *p* value less than 0.05 ($p < 0.05$) was considered statistically significant.

Standard protocol approvals, registrations, and patient consent

All patients signed informed consent forms, and the study was approved by the ethics committee of the Second Affiliated Hospital of Harbin Medical University (number KY2022-188).

Results

Clinical data

The average age of the anti-NMDAR group was close to 30 years old, the others were close to 60 years old ($p = 0.005$) (Table 1). Seizures (24/32, 75%) were the most common symptom, excluding the anti-GAD65 group ($n = 2$) ($p = 0.001$). EEG, blood, and CSF analyses were performed before treatment, and all CSF bacterial and viral cultures were negative. There were statistically significant differences in EEG and CSF-TPC among the groups ($p = 0.007$, $p = 0.021$), because normal results accounted for a portion. Evidence of inflammation was verified in routine blood test results, including WBC \uparrow (12/32, 37.5%), NUET% \uparrow (22/32, 68.7%), LYMPH% \downarrow (19/32, 59.3%), and CPR \uparrow (27/32, 84.3%). Tumours were identified in 7 patients, including lung carcinoma in 6 anti-HU patients and one ovarian tumour in an anti-HU and Ri patient. The MRI was completed at a median of 8.5 days ($P_{25} = 6$, $P_{75} = 30$), and 18F-FDG PET was completed at a median of 30 days ($P_{25} = 14$, $P_{75} = 60$). There was a significant difference in the duration of symptoms to imaging between MRI and 18F-FDG PET/CT ($p = 0.001$).

The proportion of patients with an mRS score of 4 (37.5%, 12/32) was the highest before treatment. All patients accepted the first line of treatment, and long-term immune treatment was performed in four patients (anti-LGI1, anti-GAD65, anti-CASPR2, anti-GFAP) ($p = 0.047$). The prognosis was obviously improved, and the mRS score of 1 (37.5%, 12/32) was dramatically decreased after treatment (Fig. 2). Due to the death of tumours, the mRS scores after treatment at the last follow-up were higher in the anti-HU group ($p = 0.001$).

Comparisons among MRI, visual and Scenium analysis of 18F-FDG PET findings in case groups

We observed accordance analysis results on MRI and 18F-FDG PET and compared them (Table 2). The proportion of abnormal MRI findings was 32.2% (10/31), whereas that of 18F-FDG PET was 95.5% (21/22) ($P = 0.001$) (Fig. 3). Following the principle of symmetrical distribution of brain metabolism and calculating AI, visual assessment of 18F-FDG PET showed abnormalities of the temporal lobes (mainly infringing on the hippocampus and amygdala) in 17 patients, the basal ganglia

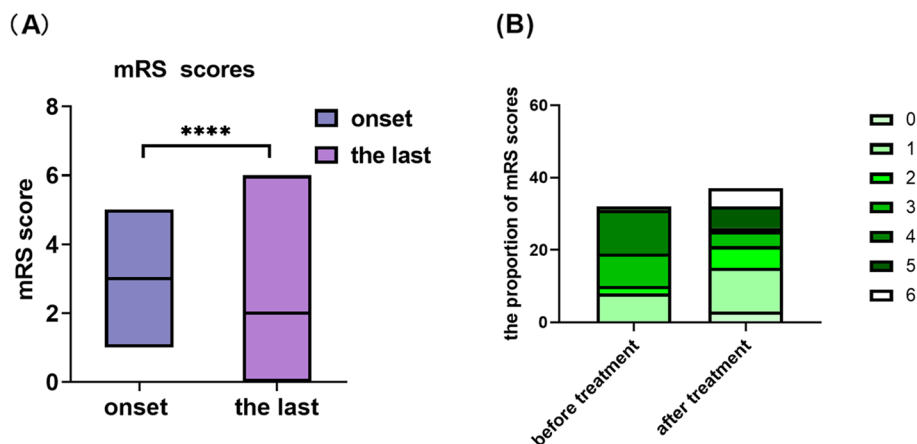


Fig. 2 **A** The mRS scores of onset and the last follow up. The median of mRS score after treatment was lower than the onset, and it had significant statistical difference ($p=0.001$). **B** The mRS score of 4 (37.5%, 12/32) was the most proportion before treatment, however, the mRS score of 1 (37.5%, 12/32) was the most proportion after treatment

in 15 patients, the frontal lobes in 9 patients, the occipital lobes in 7 patients, and the parietal lobes in 3 patients (Table 3A). Parietal lobes were more affected by anti-NMDAR than by anti-LGI1 ($p=0.036$) (Table 3B), resembling ischaemic changes caused by anti-NMDAR (No. 1, No. 2) encephalitis.

The MRI and 18F-FDG PET/CT (through Scenium analysis) manifestations in the case groups are summarized in (Table 4). The 18F-FDG PET result was negative in one patient (No. 21), and a single abnormal uptake region was observed in 5 patients, three involving the hippocampus (No. 13, No. 14, No. 27), one each involving the basal ganglia (No. 23) and the cingulate gyrus (No. 26). Multiple abnormal uptakes of cortical regions were observed in 16 patients.

Comparison of BRRM SUVs between case and control groups

As for the SUV_{max} , the results revealed significantly high uptakes of the left inferior frontal gyrus (orbital part), left inferior and middle temporal gyri in the anti-GABABR group compared with the certain group ($p=0.029$, $p=0.023$, $p=0.04$), and the results of the former group were higher. There was a significant difference ($p=0.023$) in the right fusiform gyrus between the anti-GABABR and anti-NMDAR groups (Fig. 4, Supplemental Fig. 1).

For the SUV_{mean} , hypermetabolism of the bilateral hippocampus and amygdala were significantly different (left $p=0.033$, right $p=0.029$) between the anti-GABABR group and the certain group, accompanied by higher SUVs in the anti-GABABR group. The hypometabolism of the right middle occipital gyrus was

significantly different between the anti-NMDAR and anti-LGI1 groups ($p=0.018$), with that being lower in the former group. There were significant differences in the left supramarginal gyrus and right parietal lobe in the anti-GABABR group, the anti-HU group ($p=0.016$), and the certain group ($p=0.030$); the former was lower.

The SUV_{mean} and SUV_{max} of the parietal and occipital lobes in the anti-NMDAR group were lower than those in control group-1, without hypermetabolism of the frontal lobe. The difference was the hypermetabolism of the unilateral hippocampus and cingulate gyrus in patient (No. 2). The other groups were also compared with control group-2, and the top four affected sites were the MTL (hippocampus), basal ganglia, other parts of the temporal lobe, and frontal lobe.

18F-FDG PET parameters to predict the severity of this disorder and evaluate the prognosis

As confirmed, the increased mRS scores before and after treatment might be associated with the number of lesions on 18F-FDG PET before treatment ($P>0.05$). The correlations were positive, which was more significant before the treatment (Fig. 5), (Table 5). It is necessary to find evidence from the SUVs of case groups to evaluate the severity of this disorder before treatment. The SUV_{mean} and SUV_{max} of the unilateral parietal (SUV_{mean} , $R^2=0.05$, $p>0.05$) and occipital lobes (SUV_{mean} , $R^2=0.082$, $p>0.05$) were negatively correlated with the mRS scores before treatment (Fig. 6A, Supplemental Fig. 2), and the SUV_{mean} of the unilateral superior temporal gyrus, caudate nucleus, cingulate gyrus, paracingulate gyrus, and frontal gyrus were

Table 2 The comparison between 18F-FDG PET and MRI diagnosis

Patient number	Antibody type	Sex	Age (years)	18F-FDG PET diagnoses	18F-FDG PET delay (days)	MR diagnoses	MR delay (days)	Accordance between 18F-FDG PET and MR
1	NMDAR	Female	36	Encephalitis	30	Encephalitis	20	Yes
2	NMDAR	Male	34	Encephalitis	20	Encephalitis	20	Yes
3	NMDAR	Female	13	—	—	Normal	8	—
4	NMDAR	Female	14	—	—	Demyelination	3	—
5	NMDAR	Male	25	—	—	—	—	—
6	NMDAR	Female	25	—	—	Normal	60	—
7	LGI1	Female	64	Encephalitis	30	Encephalitis	4	Yes
8	LGI1	Female	56	—	—	Normal	9	—
9	LGI1	Male	67	—	—	Normal	60	—
10	LGI1	Female	61	—	—	Normal	90	—
11	LGI1	Male	54	Encephalitis	21	Normal	11	No
12	LGI1	Female	40	Encephalitis	6	Normal	2	No
13	LGI1	Male	54	Encephalitis	30	Encephalitis	1	Yes
14	LGI1	Male	55	Encephalitis	30	Normal	30	No
15	GABABR	Male	41	—	—	Encephalitis	14	—
16	GABABR	Male	66	Encephalitis	30	Encephalitis	1	Yes
17	GABABR	Female	56	Encephalitis	24	Normal	21	No
18	GABABR	Male	64	Encephalitis	16	Normal	5	No
19	GABABR	Male	57	Encephalitis	14	Normal	1	No
20	HU	Female	55	Encephalitis	14	Normal	1	No
21	HU	Female	67	Normal	183	Normal	150	No
22	HU	Male	77	Encephalitis	30	Normal	30	No
23	HU	Female	60	Encephalitis	90	Normal	90	No
24	SOX1 and HU	Female	51	Encephalitis	60	Encephalitis	30	No
25	SOX1 and HU	Female	63	Encephalitis	14	Normal	7	No
26	HU and RI	Female	66	Encephalitis	183	Normal	7	No
27	GAD65-Ab+	Female	64	Encephalitis	60	Encephalitis	50	Yes
28	GAD65-Ab+	Female	55	Encephalitis	300	Normal	300	No
29	PNMA2+ /Ma2/Ta	Female	48	Encephalitis	14	Encephalitis	2	Yes
30	Amphiphysin	Male	63	Encephalitis	7	Normal	1	No
31	CASPR2	Male	55	—	—	Normal	14	—
32	GFAP	Female	35	—	—	Encephalitis	7	—

Abbreviations: 18F-FDG PET 2-deoxy-2-[18F]fluoro-D-glucose positron emission tomography, MRI magnetic resonance imaging, NMDAR N-methyl-D-aspartate receptor, LGI1 leucine-rich glioma inactivated-1, CASPR2 contacting-associated protein-2, GABABR gamma-aminobutyric acid receptor, AMPAR α -amino-3-hydroxy-5-methyl-4-isoxazole propionic acid receptor, GAD65 glutamic acid decarboxylase

positively correlated. The SUV_{max} of the bilateral or unilateral basal ganglia (especially the lenticular nucleus and pallidum), amygdala, and frontal gyrus (orbital part) were positively correlated with the mRS scores before treatment, and the SUV_{mean} of the left occipital lobe was the most remarkable result.

With respect to prognosis. The SUV_{mean} and SUV_{max} of the MTL, frontal lobe, basal ganglia and parietal lobes before treatment on 18F-FDG PET were positively correlated with the mRS scores after treatment (Fig. 6B, Supplemental Fig. 3), and the SUV_{max} of the MTL was the most notable result ($R^2=0.1471$, $p>0.05$) factor.

Discussion

There were three major highlights and clinical implications in our study. First, it was revealed that the most vulnerable site was the MTL (especially the hippocampus) in AE patients, which showed hypermetabolism by semi-quantitative brain 18F-FDG PET. The results were more convincing because of the large number of controls. The basal ganglia was the second most involved area, which was typical in anti-GABABR, LGI1, HU, and PNMA2+ /Ma2/Ta types in our study. The results of other lobes metabolism were as follows: the metabolism of the frontal lobe in the anti-GABABR group was higher,

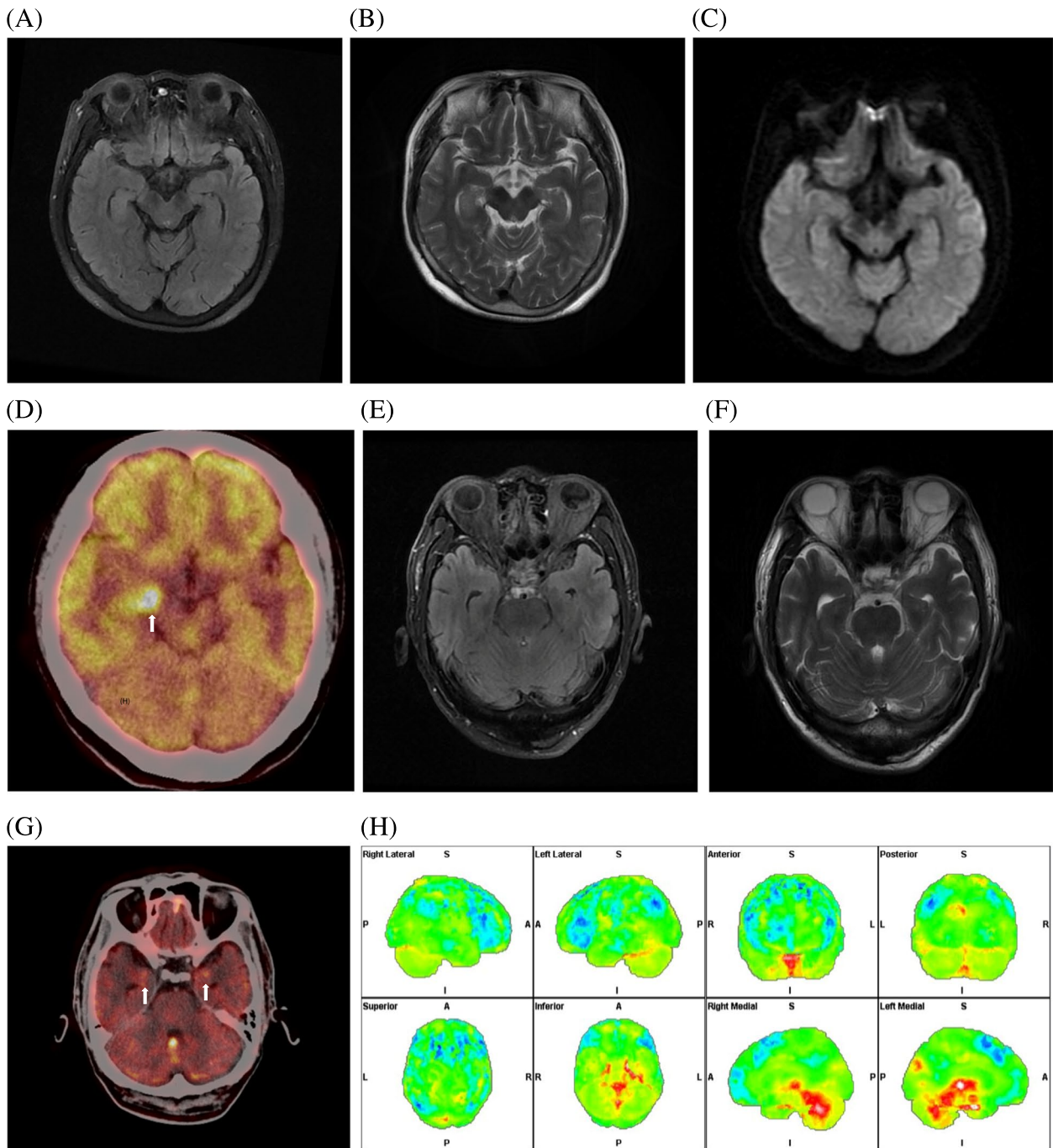


Fig. 3 No.17, anti-GABABR patient, female, 56 years old, accompanying with seizures for 2 weeks, with negative MR and positive PET manifestations. **A-C** bilateral hippocampus in axial FLAIR, T2WI and DWI in MRI showed normal signal. **D** Hypermetabolism of right hippocampus in 18F-FDG PET (thick white arrow). No.18, anti-GABABR patient, male, 64 years old, with seizures for 2 weeks, with negative MR and positive PET manifestations. **E and F** bilateral hippocampus in axial FLAIR and T2WI in MRI showed normal signal. **G** Hypermetabolism of bilateral hippocampus in 18F-FDG PET (thick white arrow). **H** Through the Scenium software analysis, the bilateral MTL showed hypermetabolism in 18F-FDG PET compared with the normal group, the Standard Deviation from SUV_{mean} was 11.8 (left) and 6.5 (right) respectively

and the SUV_{mean} and SUV_{max} of the parietal and occipital lobes were lower than controls in the anti-NMDAR group, which were in accordance with the results of Liu

X et al. [18] and multiple studies related to anti-NMDAR [19–22]. Second, it was confirmed that 18F-FDG PET can show abnormalities with more sensitivity than MRI

Table 3 Visual assessment on 18F-FDG PET: affected lobes with regions of hyper and/or hypometabolism and increased uptake in basal ganglia

Affected lobes	Anti-NMDAR	Anti-GABABR	Anti-LGI1	Anti-HU	Anti-GAD65	Anti-PNMA2+ / Ma2/ta	Anti-Amphiphysin
A: Patient details							
Total cases	N=2	N=4	N=6	N=7	N=3	N=1	N=1
Frontal anomalies	2	1	1	5	0	0	0
Temporal anomalies	2	4	3	4	2	1	1
Parietal anomalies	2	0	0	0	0	1	0
Occipital anomalies	1	0	1	2	2	0	1
Increased basal ganglia	0	1	5	5	2	1	1
B: Statistical analysis							
Frontal lobes	Anti-NMDAR	Anti-GABABR	Anti-LGI1	Anti-HU	Anti-GAD65		
Anti-GABABR	<i>p</i> =0.40						
Anti-LGI1	<i>p</i> =0.464	<i>p</i> =1.00					
Anti-HU	<i>p</i> =1.00	<i>p</i> =0.242	<i>p</i> =0.103				
Anti-GAD65	<i>p</i> =0.40	<i>p</i> =1.00	<i>p</i> =1.00	<i>p</i> =0.167			
Anti-the certain group	<i>p</i> =1.00	<i>p</i> =1.00	<i>p</i> =1.00	<i>p</i> =0.167	<i>p</i> =1.00		
Temporal lobes	Anti-NMDAR	Anti-GABABR	Anti-LGI1	Anti-HU	Anti-GAD65		
Anti-GABABR	<i>p</i> =1.00						
Anti-LGI1	<i>p</i> =0.464	<i>p</i> =0.20					
Anti-HU	<i>p</i> =0.50	<i>p</i> =0.234	<i>p</i> =1.00				
Anti-GAD65	<i>p</i> =1.00	<i>p</i> =0.429	<i>p</i> =1.00	<i>p</i> =1.00			
Anti-the certain group	<i>p</i> =1.00	<i>p</i> =1.00	<i>p</i> =0.50	<i>p</i> =0.167	<i>p</i> =1.00		
Parietal lobes	Anti-NMDAR	Anti-GABABR	Anti-LGI1	Anti-HU	Anti-GAD65		
Anti-GABABR	<i>p</i> =0.067						
Anti-LGI1	<i>p</i> =0.036*	<i>p</i> =1.00					
Anti-HU	<i>p</i> =0.083	<i>p</i> =1.00	<i>p</i> =1.00				
Anti-GAD65	<i>p</i> =0.1	<i>p</i> =1.00	<i>p</i> =1.00	<i>p</i> =1.00			
Anti-the certain group	<i>p</i> =0.33	<i>p</i> =1.00	<i>p</i> =0.50	<i>p</i> =1.00	<i>p</i> =1.00		
Occipital lobes	Anti-NMDAR	Anti-GABABR	Anti-LGI1	Anti-HU	Anti-GAD65		
Anti-GABABR	<i>p</i> =0.33						
Anti-LGI1	<i>p</i> =0.464	<i>p</i> =0.048*					
Anti-HU	<i>p</i> =1.00	<i>p</i> =0.061	<i>p</i> =1.00				
Anti-GAD65	<i>p</i> =1.00	<i>p</i> =0.429	<i>p</i> =0.226	<i>p</i> =0.50			
Anti-the certain group	<i>p</i> =1.00	<i>p</i> =0.333	<i>p</i> =0.464	<i>p</i> =1.00	<i>p</i> =1.00		
Basial ganglia	Anti-NMDAR	Anti-GABABR	Anti-LGI1	Anti-HU	Anti-GAD65		
Anti-GABABR	<i>p</i> =1.00						
Anti-LGI1	<i>p</i> =0.107	<i>p</i> =0.190					
Anti-HU	<i>p</i> =0.167	<i>p</i> =0.242	<i>p</i> =1.00				
Anti-GAD65	<i>p</i> =0.40	<i>p</i> =0.486	<i>p</i> =1.00	<i>p</i> =1.00			
Anti-the certain group	<i>p</i> =0.333	<i>p</i> =0.40	<i>p</i> =1.00	<i>p</i> =1.00	<i>p</i> =1.00		

Abbreviations: 18F-FDG PET 2-deoxy-2-[18F]fluoro-D-glucose positron emission tomography, NMDAR N-methyl-D-aspartate receptor, LGI1 leucine-rich glioma inactivated-1, CASPR2 contacting-associated protein-2, GABABR gamma-aminobutyric acid receptor, AMPAR α-amino-3-hydroxy-5-methyl-4-isoxazole propionic acid receptor, GAD65 glutamic acid decarboxylase

* *p*=0.036*: the metabolism results through visual assessment of parietal lobes was statistically significant between anti-NMDAR group and anti-LGI1 group. *p*=0.048*: The metabolism results through visual assessment of occipital lobes was statistically significant between anti-GABABR group and anti-LGI1 group

in most AE patients. A review of the literature identified 139 patients with AE, 86% with abnormal 18F-FDG PET findings and MRI findings in 59.6% (68/114) [23],

whereas there was no MRI abnormality in 10–25% of patients [24]. 18F-FDG PET seems more meticulous and precise.

Table 4 The detailed MRI and 18F-FDG PET/CT (through Scenium analysis) results of AE patients

Patient number	Antibody type	Gender	Age	MRI results T2WI/Flair/perfusion hyper-intensities	18F-FDG PET results of Scenium analysis	
					Hyper metabolism	Hypo metabolism
1	NMDAR	Female	36	Right cerebrum, brainstem, right thalamus and basal ganglia	Right supplementary motor area and middle cingulate	Right frontal, temporal, parietal, occipital lobes and left parietal lobe
2	NMDAR	Male	34	Right frontal, parietal, temporal lobe, especially temporal lobe	Right frontal, temporal, insula lobe and anterior and middle cingulate left hippocampus and brainstem	Bilateral parietal lobe and occipital lobe, left frontal lobe
3	NMDAR	Female	13	Normal	—	
4	NMDAR	Female	14	Demyelination	—	
5	NMDAR	Male	25	—	—	
6	NMDAR	Female	25	Normal	—	
7	LGI1	Female	64	Left temporal and occipital lobe, left hippocampus and brainstem	Bilateral basal ganglia, amygdala, hippocampus, para- hippocampus and anterior cingulate	
8	LGI1	Female	56	Normal	—	
9	LGI1	Male	67	Normal	—	
10	LGI1	Female	61	Normal	—	
11	LGI1	Male	54	Normal	Bilateral basal ganglia, amygdala, hippocampus, para- hippocampus and anterior cingulate	
12	LGI1	Female	40	Normal	Bilateral basal ganglia, amygdala, hippocampus, para- hippocampus and anterior cingulate	
13	LGI1	Male	54	Bilateral hippocampus, insula and temporal lobe	Bilateral hippocampus and insula	
14	LGI1	Male	55	Normal	Bilateral hippocampus and insula	
15	GABABR	Male	41	Left hippocampus, basal ganglia and temporal lobe	—	
16	GABABR	Male	66	Bilateral hippocampus, insula and temporal lobe	Bilateral basal ganglia, amygdala, hippocampus, para- hippocampus	
17	GABABR	Female	56	Normal	Bilateral basal ganglia, amygdala, hippocampus, para-hippocampus, anterior and middle cingulate, right insula and inferior frontal gyrus	
18	GABABR	Male	64	Normal	Bilateral hippocampus and thalamus	
19	GABABR	Male	57	Normal	Bilateral basal ganglia, amygdala, hippocampus, para-hippocampus	
20	HU	Female	55	Normal	Bilateral basal ganglia, amygdala, left hippocampus, para- hippocampus, bilateral anterior cingulate, right central region and right gyrus rectus and cuneus gyrus	
21	HU	Female	67	Normal	Normal	
22	HU	Male	77	Normal	Bilateral basal ganglia, amygdala, left hippocampus, para- hippocampus, right orbital gyrus, bilateral central region and anterior central gyrus and brainstem	
23	HU	Female	60	Normal	Bilateral basal ganglia	
24	SOX1 and HU	Female	51	Bilateral hippocampus, left insula and temporal lobe	Bilateral basal ganglia, amygdala, hippocampus, para- hippocampus, left paracentral lobe and brainstem	

Table 4 (continued)

Patient number	Antibody type	Gender	Age	MRI results T2WI/Flair/perfusion hyperintensities	18F-FDG PET results of Scenium analysis	
					Hyper metabolism	Hypo metabolism
25	SOX1 and HU	Female	63	Normal	Bilateral amygdala, hippocampus, para-hippocampus, left paracentral lobe, left lingual gyrus and bilateral occipital lobe	
26	HU and RI	Female	66	Normal	Bilateral cingulate gyrus	
27	GAD65-Ab+	Female	64	Bilateral hippocampus, insula and temporal lobe	Bilateral amygdala, hippocampus	
28	GAD65-Ab+	Female	55	Normal	Bilateral parietal and occipital lobe, bilateral paracentral lobe, left hippocampus, para-hippocampus	
29	PNMA2+ /Ma2/Ta	Female	48	Left temporal and parietal lobe, left insula and hippocampus	Bilateral amygdala, hippocampus, para-hippocampus, insula and anterior central gyrus, left basal ganglia, cingulate gyrus, olfactory cortex	Left temporal and parietal lobe
30	Amphiphysin	Male	63	Normal	Bilateral occipital lobe and thalamus, anterior central gyrus	
31	CASPR2	Male	55	Normal	—	—
32	GFAP	Female	35	Right temporal and occipital lobe, right cerebellum	—	—

Abbreviations: AE Autoimmune Encephalitis, 18F-FDG PET 2-deoxy-2-[18F]fluoro-D-glucose positron emission tomography, MRI magnetic resonance imaging, NMDAR N-methyl-D-aspartate receptor, LGI1 leucine-rich glioma inactivated-1, CASPR2 contacting-associated protein-2, GABABR gamma-aminobutyric acid receptor, AMPAR α -amino-3-hydroxy-5-methyl-4-isoxazole propionic acid receptor, GAD65 glutamic acid decarboxylase 65

Third and most importantly, 18F-FDG PET parameters were used to evaluate the severity degree and prognosis. The numbers of focuses on 18F-FDG PET before treatment were more important factors in association with the mRS scores before and after treatment, which was rarely reported in previous literature. It is easy to explain that the more parts of the cerebral cortex involved, the worse the ability to recover function, as seen in our anti-NMDAR and anti-PNMA2+ /Ma2/Ta patients who developed encephalitis. Hypermetabolism of the MTL was common in imaging diagnosis, accompanied by hypometabolism of occipital or parietal lobes. This feature aggravates the severity of this disorder. We also found that the SUV_{max} of the MTL was the most notable factor associated with the mRS scores after treatment.

The hypermetabolism of the MTL was the most remarkable feature in our study diagnosed with anti-GABABR, LGI1, HU, anti-Ma and anti-Ta, and anti-NMDAR encephalitis, which was similar to prior reports [18, 19, 25–30]. The SUV_{mean} of the MTL in the anti-GABABR group was higher than that in the other groups, which might be a reminder that the former more easily involves the MTL. Meanwhile, this manifestation might combine to trigger different types of tumours in the anti-HU group, which was confirmed in

this study. Metabolic changes on 18F-FDG PET in the extralimbic regions, consisting of the basal ganglia and occipital, parietal, and frontal lobes. Our three patients in the anti-LGI1 group, who also had faciobrachial dystonic seizures (FBDs); two patients in the anti-GAD65 group; and four patients in the anti-HU group without focal motor status epilepticus (FMSE) all showed hypermetabolism of the basal ganglia, which was as described in the previous literature [31–36]. The different viewpoint was that Valerio Frazzini et al. [37] studied anti-HU patients with FMSE.

It is worth noting that multiple focal infiltrates of inflammatory cells lead to the development of neuronal hyperexcitability and that myoclonic jerks may arise from an atypical propagation of neuronal activity along various networks. Such propagation may differ from that observed in typical motor seizures, resembling the FBDS [38]. Our anti-NMDAR cases without basal ganglia hypermetabolism resemble those reported by Tripathi et al. [39]. In general, neocortical hypometabolism may result from functional impairment propagated along cortical and subcortical networks arising from the sites of primary abnormalities in the MTL and basal ganglia [40]. Overall, hypermetabolism of the MTL and basal ganglia on 18F-FDG PET may be referred as a marker of neuroinflammation in some types of AE [13, 16, 25].

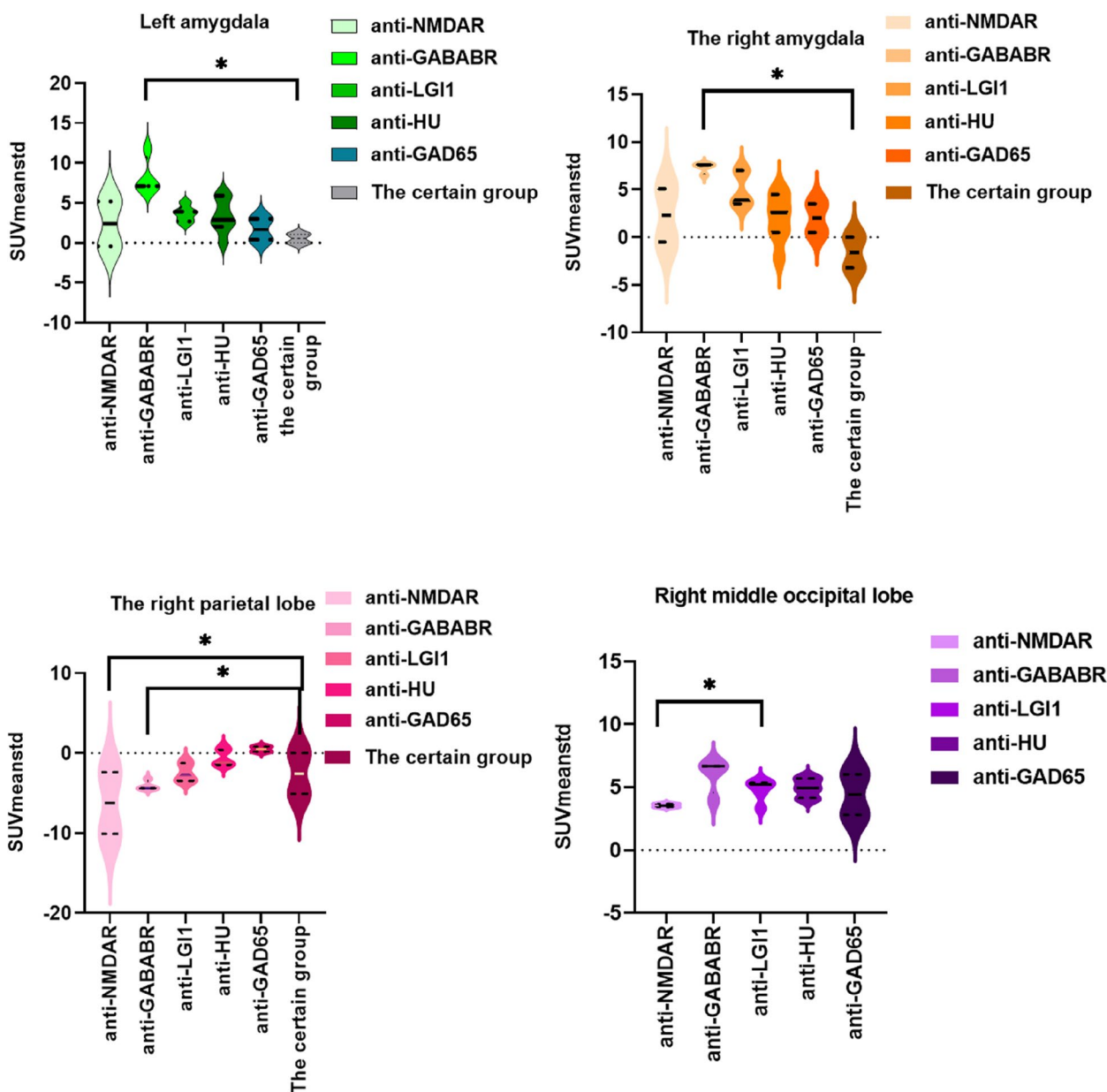


Fig. 4 Results of comparative BRRM across different sites in the case groups

Generally, previous studies [41, 42] have demonstrated that older age, tumours, and convulsive status epilepticus are related to poor prognosis. Liu X et al. [18] and Xinyue Zhang et al. [42] found involvement of the limbic system in the anti-GABAB group on 18F-FDG PET and MRI, which was more common in the poor prognosis group than in the favourable prognosis group, contrary to the viewpoint of Qian Zhao et al. [43] in LGI1 encephalitis. However, in our study, the SUV_{max} of the MTL was the most notable result in six types of AE for prognosis, which was different from

one type of antibody. Future prospective studies will be required to verify these findings and explore pathogenic mechanisms.

This study is limited by its retrospective nature and selection bias. Twenty-two patients only underwent 18F-FDG PET in the acute and subacute phases of disease, and two patients with anti-LGI1 and anti-GAD65 group underwent 18F-FDG PET after 1 year of treatment; thus, it will be difficult to evaluate treatment effects. Further prospective and longitudinal cohort studies should be performed.

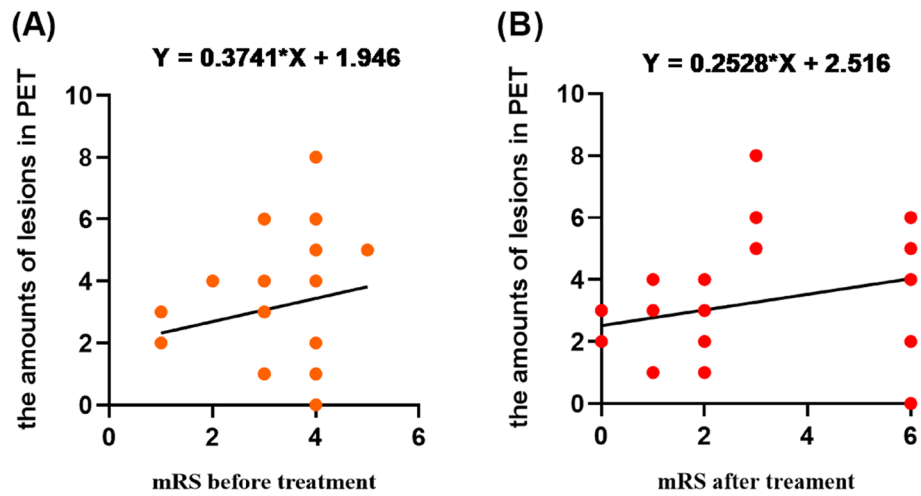


Fig. 5 **A** The positive correlation between the amounts of lesions in PET and mRS score before treatment; **B** The positive correlation between the amounts of lesions in PET and mRS score after treatment; however, the former was significant than the latter

Table 5 The detailed descriptions of the mRS score before treatment, the mRS score after treatment and the number of lesions on 18F-FDG PET of AE patients

Patient number	Antibody type	Sex	Age (years)	The mRS score before treatment	The mRS score after treatment	The number of lesions on 18F-FDG PET
1	NMDAR	Female	36	4	3	8
2	NMDAR	Male	34	4	3	6
3	LGI1	Female	64	3	2	3
4	LGI1	Male	54	1	0	3
5	LGI1	Female	40	1	0	3
6	LGI1	Male	54	4	1	1
7	LGI1	Male	55	3	1	1
8	GABABR	Male	66	4	6	2
9	GABABR	Female	56	3	6	4
10	GABABR	Male	64	4	2	2
11	GABABR	Male	57	1	5	2
12	HU	Female	55	3	6	6
13	HU	Female	67	4	6	0
14	HU	Male	77	4	6	5
15	HU	Female	60	3	2	1
16	SOX1 and HU	Female	51	4	2	4
17	SOX1 and HU	Female	63	4	6	4
18	HU and RI	Female	66	3	1	1
19	GAD65-Ab+	Female	64	3	1	1
20	GAD65-Ab+	Female	55	2	1	4
21	PNMA2 + /Ma2/Ta	Female	48	5	3	5
22	Amphiphysin	Male	63	3	1	3

Abbreviations: AE Autoimmune Encephalitis, 18F-FDG PET 2-deoxy-2-[18F]fluoro-D-glucose positron emission tomography, mRS modified Rankin Scale, NMDAR N-methyl-D-aspartate receptor, LGI1 leucine-rich glioma inactivated-1, GABABR gamma-aminobutyric acid receptor, GAD65 glutamic acid decarboxylase 65

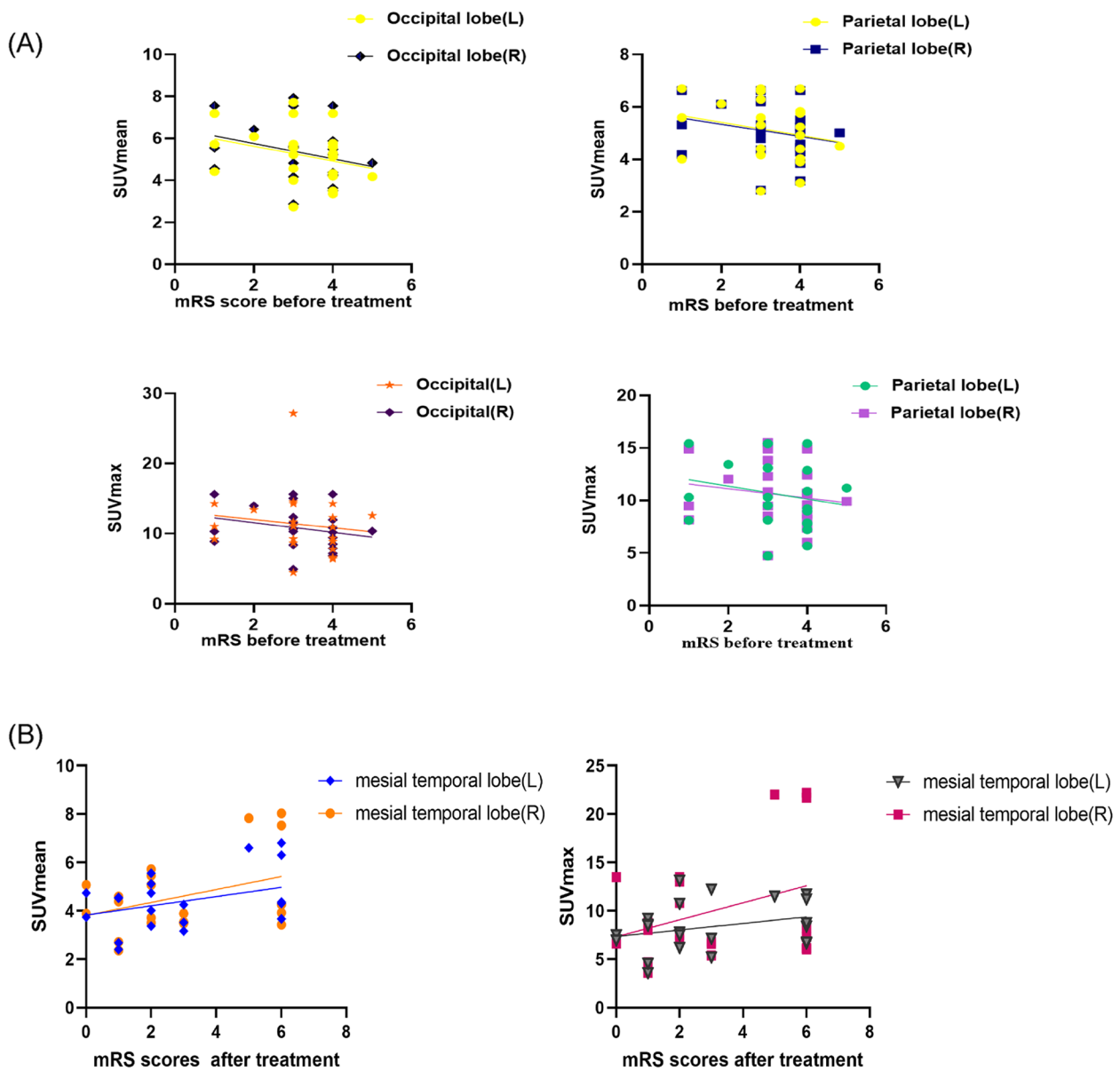


Fig. 6 **A** Simple linear regression, to evaluate the relationship among SUV_{mean} and SUV_{max} of BRRM and mRS scores before treatment. SUV_{mean} and SUV_{max} of parietal and occipital lobe had the negative correlation. **B** Simple linear regression, to evaluate the relationship among SUV_{mean} and SUV_{max} of BRRM and mRS scores after treatment. SUV_{mean} and SUV_{max} of MTL had the positive correlation with the mRS score after treatment

Conclusions

In summary, this study provided detailed descriptions of distinct cerebrum metabolic patterns related to acute and subacute phases of AE on 18F-FDG PET, which was more sensitive than MRI. The common pattern of AE was high MTL metabolism on 18F-FDG PET, which was associated with a decreasing SUV_{mean} of the occipital lobe, and the number of lesions on PET before treatment may be significant factors in assessing disease severity. The increasing SUV_{max} of the MTL may serve as a prognostic

biomarker in AE. Future prospective studies are required to verify these manifestations and to identify more accurate prognostic factors.

Abbreviations

- AE Autoimmune Encephalitis
- 18F-FDG PET 2-Deoxy-2-[18F]fluoro-D-glucose positron emission tomography
- MRI Magnetic Resonance Imaging
- AAL Anatomical Automatic Labeling
- mRS Modified Rankin Scale
- MTL Mesial Temporal Lobe

SUV _{mean}	Mean standardized uptake value
SUV _{max}	Max standardized uptake value
SUV _{meanstd}	Standardized deviation from the SUV _{mean}
SUV _{maxstd}	Standardized deviation from the SUV _{max}
HSV	Herpes simplex virus
ICIs	Immune-checkpoint inhibitors
CRP	C-reactive protein
CSF	Cerebrospinal fluid
TPC	Total protein counts
EEG	Electroencephalogram
WBC	White Blood Cell
CEA	Carcinoembryonic antigen, the normal value < 5 ng/mL
SCC	Squamous cell carcinoma antigen, the normal value < 1.5 ng/mL
CYFRA21-1	Cytokeratin-19-fragment, the normal value < 2.5 ng/mL
NSE	Neuron-specific enolase, the normal value < 17 ng/mL
CA125	The normal value < 35U/ml
CA199	The normal value < 37U/ml
AED	Anti-epileptic drugs; The first line of treatment included steroids, IVlg, and plasma exchange; Long immune treatment included Mycophenolate Mofetil and Azathioprine; The certain group: included four patients, anti-PNMA2+/Ma2/ta, anti-Amphiphysin, anti-CASPR2, anti-GFAP, respectively one case, however, only anti-PNMA2+/Ma2/ta, anti-Amphiphysin performed PET examination
NMDAR	N-methyl-D-aspartate receptor
LGI1	Leucine-rich glioma inactivated-1
CASPR2	Contacting-associated protein-2
GABABR	Gamma-aminobutyric acid receptor
AMPA	α-Amino-3-hydroxy-5-methyl-4-isoxazole propionic acid receptor
GAD65	Glutamic acid decarboxylase 65
BRRM	Brain relative regional metabolism
T1WI	T1 weighted image
T2WI	T2 weighted image
FLAIR	Fluid attenuated inversion recovery
TR	Repetition time
TE	Echo time
FOV	Field of view
AI	Asymmetric Index
FBDs	Faciobrachial Dystonic Seizure
FMSE	Focal Motor Status Epilepticus

Supplementary Information

The online version contains supplementary material available at <https://doi.org/10.1186/s12880-023-01148-6>.

Additional file 1: Supplemental Fig. 1 Other results of comparative BRRM across different sites in the case groups. **Supplemental Fig. 2** Simple linear regression, to evaluate the relationship among SUV_{mean} and SUV_{max} of BRRM and mRS scores before treatment, superior temporal lobe(R), caudate nucleus(R), middle frontal gyrus, orbital part (R), pallidum and basal ganglia had the positive relationship before treatment. **Supplemental Fig. 3** Simple linear regression, to evaluate the relationship among SUV_{mean} and SUV_{max} of BRRM and mRS scores after treatment. SUV_{mean} and SUV_{max} of MTL had the positive correlation with the mRS score after treatment.

Additional file 2: Supplementary Table 1. The SUV_{max} of case groups according to AAL standards. **Supplementary Table 2.** The SUV_{mean} of case groups according to AAL standards. **Supplementary Table 3.** The SUV_{maxstd} of case groups according to AAL standards. **Supplementary Table 4.** The SUV_{meanstd} of case groups according to AAL standards. **Supplementary Table 5.** The SUV_{mean} of normal 19-44 years old group according to AAL standards. **Supplementary Table 6.** The SUV_{max} of normal 19-44 years old group according to AAL standards. **Supplementary Table 7.** The SUV_{meanstd} of normal 19-44 years old group according to AAL standard. **Supplementary Table 8.** The SUV_{maxstd} of normal 19-44 years old group according to AAL standard. **Supplementary Table 9.** The SUV_{mean} of normal 45-70 years old group according to AAL standard.

Supplementary Table 10. The SUV_{max} of normal 45-70 years old group according to AAL standard. **Supplementary Table 11.** The SUV_{meanstd} of normal 45-70 years old group according to AAL standard. **Supplementary Table 12.** The SUV_{maxstd} of normal 45-70 years old group according to AAL standard.

Acknowledgements

Not applicable.

Author's contributions

Lili Liu and Zhehao Lyu contributed equally to this paper. The first draft of the manuscript was written by Lili Liu and Zhehao Lyu. All authors contributed to the study conception and design. Material preparation, data collection and analysis were performed by Huimin Li, Lin Bai and Yong Wan, the manuscript was revised by Ping Li. All authors read and approved the final manuscript.

Funding

The authors declare that no funds, grants, or the other support were received during the preparation of this manuscript.

Availability of data and materials

The datasets generated and analyzed during the study are not publicly available due to patient privacy, but are available from the corresponding author upon reasonable request.

Declarations

Ethics approval and consent to participate

Ethics approval was obtained from Institutional Review Board of the Second Affiliated Hospital of Harbin Medical University (number KY2022-188). All patients signed informed consent forms, especially the age under 14 years old, informed consent have been obtained from their parents. The study is a retrospective study involving human data that has already been collected and did not require additional recruitment of human subjects, waving the need for additional informed consent. All methods were carried out in accordance with relevant guidelines and regulations set by the Second Affiliated Hospital of Harbin Medical University.

Consent for publication

Written informed consents were obtained from the patients for publication of this manuscript and any accompanying images. A copy of the written consent is available for review by the Editor-in-chief of this journal.

Competing interests

The authors declare no competing interests.

Author details

¹Department of PET/CT, The Second Affiliated Hospital of Harbin Medical University, No.246 Xuefu Road, Harbin 150001, Heilongjiang, People's Republic of China. ²Department of Nuclear Medicine, The First Affiliated Hospital of Harbin Medical University, Postal Street No.23, Harbin 150001, Heilongjiang, People's Republic of China. ³Department of Nuclear Medicine, Inner Mongolia Autonomous Region People's Hospital, No.20 Zhaowuda Road, Hohhot 010017, People's Republic of China.

Received: 15 February 2023 Accepted: 31 October 2023

Published online: 20 November 2023

References

- Graus F, Titulaer MJ, Balu R, et al. A clinical approach to diagnosis of autoimmune encephalitis. *Lancet Neurol*. 2016;15:391–404.
- Dalmau J, Graus F. Antibody-mediated encephalitis. *N Engl J Med*. 2018;378:840–51.
- Heine J, Prüss H, Bartsch T, et al. Imaging of autoimmune encephalitis—relevance for clinical practice and hippocampal function. *Neuroscience*. 2015;309:68–83.

4. Singh TD, Fugate JE, Rabinstein AA. The spectrum of acute encephalitis: causes, management, and predictors of outcome. *Neurology*. 2015;84:359–66.
5. Venkatesan A, Tunkel AR, Bloch KC, et al. For the International Encephalitis Consortium. Case definitions, diagnostic algorithms, and priorities in encephalitis: consensus statement of the international encephalitis consortium. *Clin Infect Dis*. 2013;57:1114–28.
6. Dubey D, Pittcock SJ, Kelly CR, et al. Autoimmune encephalitis epidemiology and a comparison to infectious encephalitis. *Ann Neurol*. 2018;83:166–77.
7. Armangue T, Moris G, Cantarín-Extremera V, et al. Autoimmune post-herpes simplex encephalitis of adults and teenagers. *Neurology*. 2015;5(20):1736–43.
8. Kumar N, Abboud H. Iatrogenic CNS demyelination in the era of modern biologics. *Mult Scler*. 2019;25(8):1079–85.
9. Höftberger R, Titulaer MJ, Sabater L, et al. Encephalitis and GABAB receptor antibodies: novel findings in a new case series of 20 patients. *Neurology*. 2013;81(17):1500–6. <https://doi.org/10.1212/WNL.0b013e3182a9585f>.
10. Graus F, Escudero D, Oleaga L, et al. Syndrome and outcome of antibody-negative limbic encephalitis. *Eur J Neurol*. 2018;25(8):1011–6. <https://doi.org/10.1111/ene.13661>.
11. Budhram A, Leung A, Nicolle MW, Burneo JG. Diagnosing autoimmune limbic encephalitis. *CMAJ*. 2019;191(19):E529–34. <https://doi.org/10.1503/cmaj.181548>.
12. Solnes LB, Jones KM, Rowe SP, et al. Diagnostic value of 18F-FDG PET/CT versus MRI in the setting of antibody-specific autoimmune encephalitis. *J Nucl Med*. 2017;58(8):1307–13.
13. Turpin S, Martineau P, Levesseur MA, et al. 18F-fluorodeoxyglucose positron emission tomography with computed tomography (FDG PET/CT) findings in children with encephalitis and comparison to conventional imaging. *Eur J Nucl Med Mol Imaging*. 2019;46(6):1309–24.
14. Muzik O, Chugani DC, Shen C, et al. Objective method for localization of cortical asymmetries using positron emission tomography to aid surgical resection of epileptic foci. *Comput Aided Surg*. 1998;3(2):74–82. [https://doi.org/10.1002/\(SICI\)1097-0150\(1998\)3:2%3C74::AID-IGS4%3E3.0.CO;2-H](https://doi.org/10.1002/(SICI)1097-0150(1998)3:2%3C74::AID-IGS4%3E3.0.CO;2-H).
15. Zhang Q, Liao Y, Wang X, et al. A deep learning framework for 18F-FDG PET imaging diagnosis in pediatric patients with temporal lobe epilepsy. *Eur J Nucl Med Mol Imaging*. 2021;48(8):2476–85. <https://doi.org/10.1007/s00259-020-05108-y>.
16. Dragogna F, Mauri MC, Marotta G, Armao FT, Brambilla P, Altamura AC. Brain metabolism in substance-induced psychosis and schizophrenia: a preliminary PET study. *Neuropsychobiology*. 2014;70(4):195–202. <https://doi.org/10.1159/000366485>.
17. Tzourio-Mazoyer N, Landeau B, Papathanassiou D, et al. Automated anatomical labeling of activations in SPM using a macroscopic anatomical parcellation of the MNI MRI single-subject brain. *Neuroimage*. 2002;15(1):273–89. <https://doi.org/10.1006/nimg.2001.0978>.
18. Liu X, Yu T, Zhao X, et al. 18F-fluorodeoxyglucose positron emission tomography pattern and prognostic predictors in patients with anti-GABAB receptor encephalitis. *CNS Neurosci Ther*. 2022;28(2):269–78.
19. Moubtakir A, Dejust S, Godard F, et al. 18F-FDG PET/CT in anti-NMDA receptor encephalitis: typical pattern and follow-up. *Clin Nucl Med*. 2018;43(7):520–1.
20. Maeder-Ingvar M, Prior JO, Irani SR, et al. FDG-PET hyperactivity in basal ganglia correlating with clinical course in anti-NMDAR antibodies encephalitis. *J Neurol Neurosurg Psychiatry*. 2011;82(2):235–6.
21. Leypoldt F, Buchert R, Kleiter I, et al. Fluorodeoxyglucose positron emission tomography in anti-N-methyl-D-aspartate receptor encephalitis: distinct pattern of disease. *J Neurol Neurosurg Psychiatry*. 2012;83(7):681–6.
22. Probasco JC, Solnes L, Nalluri A, et al. Decreased occipital lobe metabolism by FDG-PET/CT: an anti-NMDA receptor encephalitis biomarker. *Neurol Neuroimmunol Neuroinflamm*. 2018;5(1):e413.
23. Probasco JC, Solnes L, Nalluri A, et al. Abnormal brain metabolism on FDG-PET/CT is a common early finding in autoimmune encephalitis. *Neurol Neuroimmunol Neuroinflamm*. 2017;4(4):e352.
24. Van Sonderen A, Petit-Pedrol M, Dalmau J, et al. The value of LGI1, Caspr2 and voltage-gated potassium channel antibodies in encephalitis. *Nat Rev Neurol*. 2017;13(5):290–301.
25. Zhao X, Zhao S, Chen Y, et al. Subcortical hypermetabolism associated with cortical hypometabolism is a common metabolic pattern in patients with anti-leucine-rich glioma-inactivated 1 antibody encephalitis. *Front Immunol*. 2021;12:672846. <https://doi.org/10.3389/fimmu.2021.672846>.
26. Silsby M, Clarke CJ, Lee K, et al. Anti-Hu limbic encephalitis preceding the appearance of mediastinal germinoma by 9 years. *Neurol Neuroimmunol Neuroinflamm*. 2020;7(3):e685.
27. Sobas MA, Galiano Leis MA, de la Fuente CR, et al. Encefalitis límbica paraneoplásica y carcinoma epidermoide del Seno piriforme. *An Med Interna*. 2006;23(7):331–4.
28. Samejima S, Tateishi T, Arahata H, et al. A case of anti-Hu antibody- and anti-GluR epsilon2 antibody-positive paraneoplastic neurological syndrome presenting with limbic encephalitis and peripheral neuropathy. *Rinsho Shinkeigaku*. 2010;50(7):467–72.
29. Sakurai T, Wakida K, Kimura A, et al. Anti-Hu antibody-positive paraneoplastic limbic encephalitis with acute motor sensory neuropathy resembling Guillain-Barré syndrome: a case study. *Rinsho Shinkeigaku*. 2015;55(12):921–5.
30. Hoffmann LA, Jarius S, Pellkofer HL, et al. Anti-Ma and anti-Ta associated paraneoplastic neurological syndromes: 22 newly diagnosed patients and review of previous cases. *J Neurol Neurosurg Psychiatry*. 2008;79(7):767–73.
31. Moersch FP, Woltman HW. Progressive fluctuating muscular rigidity and spasm ("stiffman" syndrome); report of a case and some observations in 13 other cases. *Proc Staff Meet Mayo Clin*. 1956;31(15):421–7.
32. Solimena M, Folli F, Denis-Donini S, et al. Autoantibodies to glutamic acid decarboxylase in a patient with stiff-man syndrome, epilepsy, and type I diabetes mellitus. *N Engl J Med*. 1988;318(16):1012–20.
33. Dalakas MC, Fujii M, Li M, et al. The clinical spectrum of anti-GAD antibody-positive patients with stiff-person syndrome. *Neurology*. 2000;55(10):1531–5.
34. Wegner F, Wilke F, Raab P, et al. Anti-leucine rich glioma inactivated 1 protein and anti-N-methyl-D-aspartate receptor encephalitis show distinct patterns of brain glucose metabolism in 18F-fluoro-2-deoxy-d-glucose positron emission tomography. *BMC Neurol*. 2014;14:136. <https://doi.org/10.1186/1471-2377-14-136>.
35. Irani SR, Michell AW, Lang B, et al. Faciobrachial dystonic seizures precede Lgi1 antibody limbic encephalitis. *Ann Neurol*. 2011;69(5):892–900.
36. Shin Y-W, Lee S-T, Shin J-W, et al. VGKC complex/LGI1 antibody encephalitis: clinical manifestations and response to immunotherapy. *J Neuroimmunol*. 2013;265(1–2):75–81.
37. Frazzini V, Nguyen-Michel VH, Habert MO, et al. Focal status epilepticus in anti-Hu encephalitis. *Autoimmun Rev*. 2019;18(11):102388. <https://doi.org/10.1016/j.autrev.2019.102388>.
38. Navarro V, Kas A, Apartis E, et al. Motor cortex and hippocampus are the two main cortical targets in LGI1-antibody encephalitis. *Brain*. 2016;139(4):1079–93.
39. Tripathi M, Roy SG, Parida GK, et al. Metabolic topography of autoimmune non-paraneoplastic encephalitis. *Neuroradiology*. 2018;60(2):189–98.
40. Heine J, Prüss H, Kopp UA, et al. Beyond the limbic system: disruption and functional compensation of large-scale brain networks in patients with anti-LGI1 encephalitis. *J Neurol Neurosurg Psychiatry*. 2018;89(11):1191–9.
41. Chen W, Wang Y, Guo X, et al. A prognostic analysis of the outcomes in patients with anti-γ-aminobutyric acid B receptor encephalitis. *Front Immunol*. 2022;13:847494. <https://doi.org/10.3389/fimmu.2022.847494>.
42. Zhang X, Lang Y, Sun L, Zhang W, Lin W, Cui L. Clinical characteristics and prognostic analysis of anti-gamma-aminobutyric acid-B (GABA-B) receptor encephalitis in Northeast China. *BMC Neurol*. 2020;20(1):1. <https://doi.org/10.1186/s12883-019-1585-y>.
43. Zhao Q, Sun L, Zhao D, et al. Clinical features of anti-leucine-rich glioma-inactivated 1 encephalitis in Northeast China. *Clin Neurol Neurosurg*. 2021;203:106542. <https://doi.org/10.1016/j.clineuro.2021.106542>.

Publisher's Note

Springer Nature remains neutral with regard to jurisdictional claims in published maps and institutional affiliations.